MITIGATE THE GAP: IMPROVING CROSS-MODAL ALIGNMENT IN CLIP

Anonymous authors
Paper under double-blind review

ABSTRACT

Contrastive Language–Image Pre-training (CLIP) has manifested remarkable improvements in zero-shot classification and cross-modal vision-language tasks. Yet, from a geometrical point of view, the CLIP embedding space has been found to have a pronounced modality gap. This gap renders the embedding space overly sparse and disconnected, with different modalities being densely distributed in distinct subregions of the hypersphere. In this work, we propose AlignCLIP, in order to improve the alignment between text and image embeddings, and thereby reduce the modality gap. AlignCLIP increases the cross-modal alignment, and yields gains across several zero-shot and fine-tuning downstream evaluations by sharing the learnable parameters between the modality encoders and a semantically-regularized separation objective function on the uni-modal embeddings.

* The source code for reproducing our experiments will be released upon acceptance of the paper.

1 INTRODUCTION

One of the most prominent and widely used pre-trained vision–language models is OpenAI's Contrastive Language–Image Pre-training (CLIP) model (Radford et al., 2021). CLIP is a dual-stream vision–language encoder trained for learning a joint representation space, in which image and text modalities can be jointly embedded. It has demonstrated exceptional zero-shot capabilities for image classification, multi-modal retrieval as well as robustness to natural distribution shifts. Despite the outstanding performance of CLIP, recent work has shed light on a pronounced *modality gap* in the CLIP embedding space (Liang et al., 2022; Tyshchuk et al., 2023; Schrodi et al., 2024), leading to large distances between image and text embeddings. We illustrate these phenomena more comprehensively in Figure 1, in which the DOSNES (Lu et al., 2019) projection of the CLIP-encoded image–text pairs from CC3M (Sharma et al., 2018) using the pre-trained ViT-B-32 backend is shown. As can be seen, each modality densely populates a separate small subregion of CLIP's representation embedding space.

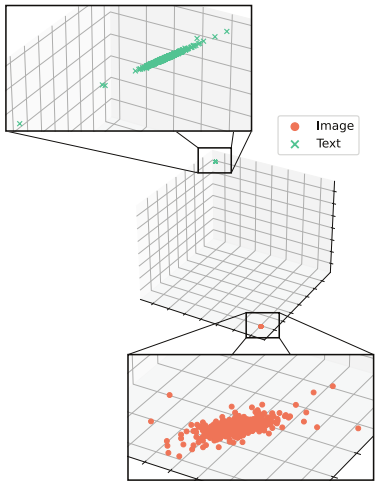

Figure 1: Modality gap in CLIP

Previous work (Liang et al., 2022; Schrodi et al., 2024; Tyshchuk et al., 2023) studied the effects of closing the gap by translating the embeddings of one of the modalities to those of the other modality, using the average distance of the image–text pairs, e.g., shifting the image embedding v_i for each image i by Δ towards the language embedding t_i, in which $\Delta = \frac{1}{N}\sum_{i=1}^{N} t_i - \frac{1}{N}\sum_{i=1}^{N} v_i$ and N is the total number of image–text pairs. However, such naive translations likely harm the relative distances of the *unpaired* images and texts, and therefore, distort the meaningful structure of the embedding space. We show this by a simple 2D example in Section A.1. In contrast, our work proposes to reduce the gap by first sharing the parameter space between the vision and language encoders and then imposing an intra-modality separation objective function. The goal of sharing

parameters between the encoders is to increase the inductive bias towards shared cross-modal encodings, and thereby, reducing the cross-modal gap. The intra-modality separation more directly aims at encouraging the embeddings within the visual modality to be reasonably expanded and pushed towards the language modality. Hence, each modality is pushed towards the embeddings of the opposite modality and thereby, the modality gap can get reduced. Our extensive experimental results support that the two aforementioned refinements show substantial improvement of the cross-modal alignment while improving the performance across a wide variety of downstream tasks.

To summarize, our contributions are as follows:

1. In Section A.1, we show that the previous naive approaches for closing the gap leads to damaged relative distances of the unpaired samples, which hurts the performance in downstream tasks.
2. Then, we propose sharing the learnable parameters of the vision and language encoders and study its effects on modality gap reduction and furthermore, on downstream performance.
3. In addition, we propose AlignCLIP, a semantically-regularized intra-modality separation objective function that enforces larger distances for the image embeddings of semantically dissimilar images, and at the same time, smaller distances on those of similar images.
4. We demonstrate that AlignCLIP achieves significant alignment of the modalities, and also substantially improves zero-shot classification, robustness to distribution shifts, and classification with linear probing.
5. We further investigate the impacts of AlignCLIP for the zero-shot and fine-tuned multi-modal retrieval tasks and provide a qualitative analysis of the image rankings as well as cosine similarities of the embeddings.

2 Background, Notations and Concepts

Given a set of N image–text pairs, we consider the CLIP image encoder f_V to obtain the l_2-normalized vector $\vec{e}_{\text{v}}^{\,i} \in \mathbb{R}^d$ as a d-dimensional embedding vector for image v_i, i.e., $f_V(v_i) = \vec{e}_{\text{v}}^{\,i}$, and the CLIP text encoder f_T to obtain the l_2-normalized text embedding $\vec{e}_{\text{t}}^{\,i} \in \mathbb{R}^d$ for the text sample t_i, i.e., $f_T(t_i) = \vec{e}_{\text{t}}^{\,i}$. We denote a batch of encoded image–text pairs by $E_{\text{v}} \in \mathbb{R}^{b\times d}$ for images and $E_{\text{t}} \in \mathbb{R}^{b\times d}$ for texts, where b refers to the batch size.

Background on CLIP. The contrastive objective in CLIP is the average of the vision to language and the language to vision Info-NCE contrastive loss functions formulated as:

$$\mathcal{L}_{v\to l} = \frac{-1}{N}\sum_{i=1}^{N}\log\frac{\exp[(\vec{e}_{\text{v}}^{\,i}\cdot\vec{e}_{\text{t}}^{\,i})\,/\,\tau]}{\sum_{j=1}^{N}\exp[(\vec{e}_{\text{v}}^{\,i}\cdot\vec{e}_{\text{t}}^{\,j})\,/\,\tau]},\quad \mathcal{L}_{l\to v} = \frac{-1}{N}\sum_{j=1}^{N}\log\frac{\exp[(\vec{e}_{\text{v}}^{\,j}\cdot\vec{e}_{\text{t}}^{\,j})\,/\,\tau]}{\sum_{i=1}^{N}\exp[(\vec{e}_{\text{v}}^{\,i}\cdot\vec{e}_{\text{t}}^{\,j})\,/\,\tau]}, \tag{1}$$

respectively, where τ is a learnable temperature parameter. The overall CLIP loss is then:

$$\mathcal{L}_{\text{clip}} = \frac{1}{2}[\mathcal{L}_{v\to l} + \mathcal{L}_{l\to v}]. \tag{2}$$

In practice, a symmetric cross-entropy loss is employed using the vision and language logits. The label $y \in \mathbb{R}$, which is the index of the image–text pair in the batch, represents the correspondence of the paired samples. For a batch of image–text pairs, $Y \in \mathbb{R}^b$ denotes the set of labels. The visual and textual logits, $\hat{y}_{\text{v}} \in \mathbb{R}^{b\times b}$ and $\hat{y}_{\text{t}} \in \mathbb{R}^{b\times b}$, are then calculated as:

$$\hat{y}_{\text{v}} = \exp(\tau)E_{\text{v}}E_{\text{t}}^{\intercal}\quad,\quad \hat{y}_{\text{t}} = \hat{y}_{\text{v}}^{\intercal}, \tag{3}$$

respectively. Ultimately, the overall CLIP loss is calculated using the cross-entropy loss, H, as:

$$\mathcal{L}_{\text{clip}} = \frac{1}{2}[H(\hat{y}_{\text{v}}, Y) + H(\hat{y}_{\text{t}}, Y)]. \tag{4}$$

Cross-Modal Alignment Score. In contrastive representation learning, the goal is to learn similar representations for positive pairs and distant representations for irrelevant negative samples. In cross-modal vision–language learning, often the paired image–texts form the positive pair distribution.

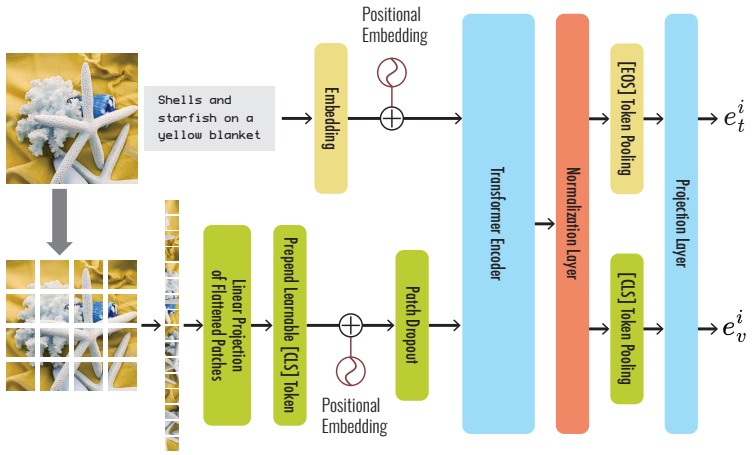

Figure 2: Overview of sharing the transformer and projection layer in SharedCLIP.

Alignment entails mapping positive pairs to close embedding vectors such that a perfect alignment is achieved when $f(x_1) = f(x_2)$ for a given encoding function f and a randomly drawn positive pair of samples x_1, x_2 (Wang & Isola, 2020). In the multi-modal scenario, we are particularly interested in studying the alignment property for the CLIP embedding space, as it represents the modality gap (Jiang et al., 2023), and therefore, we define perfect alignment as $f_T(t_i) = f_V(v_i)$.

We adopt the alignment measurement proposed by Goel et al. (2022) and define it as the average cosine similarity between the paired image and text embeddings in the CLIP embedding space:

$$\text{alignment} = \frac{1}{N}\sum_{i=1}^{N} \vec{e}_{\text{v}}^{\,i} \cdot \vec{e}_{\text{t}}^{\,i}, \qquad \text{alignment} \in [-1, 1]. \tag{5}$$

Higher scores demonstrate better alignment, and, therefore, a decrease in the modality gap.

3 AlignCLIP

We attain cross-modal alignment in AlignCLIP by two main refinements: sharing the parameter space between the vision and language encoders, as well as learning to spread out and push apart the uni-modal embeddings. The following subsections describe each of these refinements in detail.

3.1 Sharing the Learnable Parameter Space in CLIP

AlignCLIP employs a transformer-based encoder architecture (Vaswani et al., 2017), where the transformer is shared between the two vision and language modality encoders. We suspect that one of the main reasons that the modality gap exists in the original CLIP's embedding space is the fact that with a dual-stream encoder architecture, each modality has a separate disentangled set of parameters for optimization, i.e., f_T has the parameters θ and f_V has θ', which are initialized and optimized disjointly. As a result, even with the same encoder architecture for each modality, the final learned parameters θ and θ' can diverge quite radically, leading to distinct functions that map each modality to completely different subregions of the embedding space. In other words, training two transformers separately has no explicit inductive bias towards a shared region of the encoding space.

Therefore, we seek to align the outputs of the vision and language encoding functions by increasing the overlap of θ and θ' to the extent possible. We achieve this by sharing the layers of the vision and language encoding towers. Specifically, we share the transformer encoder as well as the projection layer between the vision and language modalities. Sharing the layers between the modality encoders increases the inductive bias towards a shared region of the embedding space, and therefore, reduces the modality gap. We utilize a standard transformer encoder architecture (Dosovitskiy et al., 2020). An overview of our refined overall model architecture is given in Figure 2. Yellow components are designated for the language modality, green components for the visual modality, and the blue

parts are shared between the two modalities. For encoding texts, the yellow and blue parts of the model actively contribute in the embedding calculations. Similarly, when encoding images, the green components as well as the blue ones are invoked for the computation. Following the original CLIP, we use the $[EOS]$ token pooling for text embeddings and the $[CLS]$ token embedding for the image embedding. For simplicity, we refer to this architecture as SharedCLIP throughout the rest of the paper. Sharing transformers in CLIP has been previously investigated from the perspective of downstream performance (You et al., 2022). In this work, we extend the sharing to the extent possible, i.e., we include the projection layer as well, and study the impacts with respect to the cross-modal alignment property.

3.2 Intra-Modality Separation

As shown in Figure 1, each modality resides in a distinct dense subregion of the CLIP embedding space. We hypothesize that this phenomenon is a direct result of the *cross-modal* contrastive objective in CLIP, which merely optimizes the relative distances of image embeddings and text embeddings. The cross-modal contrastive loss alone is not sufficient for imposing meaningful distances within the uni-modal embeddings, i.e., pairwise distances of text embeddings or pairwise distances of image embeddings. Therefore, we define an objective function that enforces reasonable distances within each modality by separating the uni-modal embeddings that are semantically dissimilar. In other words, we impose a semantically-regularized Intra-Modality Separation (IMSep) in addition to the CLIP's objective function.

IMSep is achieved by an InfoNCE contrastive loss, in which image–text pairs are the positive samples and all pairwise image–image combinations are considered as negative samples, respectively:

$$\mathcal{L} = \frac{-1}{N} \sum_{i=1}^{N} \log \frac{\exp[(\vec{e}_{\text{v}}^{\,i} \cdot \vec{e}_{\text{t}}^{\,i}) \,/\, \tau]}{\sum_{\substack{j=1,\\ i\neq j}}^{N} \exp[(\vec{e}_{\text{v}}^{\,i} \cdot \vec{e}_{\text{v}}^{\,j}) \,/\, \tau]}. \tag{6}$$

The distinguishing role of the IMSep loss, in comparison to the original CLIP's loss, is the enforcement of minimizing the pairwise image–image cosine similarities, i.e., the denominator in Eq. 6. As a result, this objective spreads apart different image embeddings. However, one should notice that while pushing the image embeddings away from each other, some samples might indeed bear some semantic similarity, and therefore ought not to be substantially separated. To account for this, we regularize the intra-modality separation with respect to the pairwise semantic distances of samples. Denoting the semantic distance of the image sample i from j by $\mathcal{D}_{ij}$, the regularized version of Eq. 6 becomes:

$$\mathcal{L} = \frac{-1}{N} \sum_{i=1}^{N} \log \frac{\exp[(\vec{e}_{\text{v}}^{\,i} \cdot \vec{e}_{\text{t}}^{\,i}) \,/\, \tau]}{\sum_{\substack{j=1,\\ i\neq j}}^{N} \exp[(\mathcal{D}_{ij} \cdot \vec{e}_{\text{v}}^{\,i} \cdot \vec{e}_{\text{v}}^{\,j}) \,/\, \tau]}. \tag{7}$$

In Eq. 7, the distance $\mathcal{D}_{ij}$ controls the minimization of $(\vec{e}_{\text{v}}^{\,i} \cdot \vec{e}_{\text{v}}^{\,j})$ by reducing these in-modality dot product values if the samples are semantically close (similar), and therefore, the denominator does not get strongly minimized, since the values are already small. Conversely, the denominator obtains larger values when $\mathcal{D}_{ij}$ is large, when images are semantically dissimilar, and therefore, the denominator gets strongly minimized.

In practice, IMSep aims at optimizing Eq. 7 using the cross-entropy loss. Given a batch of encoded image–text pairs, IMSep creates the $\hat{y}_{\text{vsep}}$ logits and then minimizes the cross-entropy loss over Y and $\hat{y}_{\text{vsep}}$. To this end, first the pairwise cosine similarities of the images are calculated by:

$$\mathcal{V} = E_{\text{v}} E_{\text{v}}^{\intercal}, \quad \text{where} \quad \mathcal{V} \in \mathbb{R}^{b\times b}. \tag{8}$$

For the semantic regularization, and therefore, calculating $\mathcal{D}_{ij}$, we utilize the pairing texts of the images as the semantic supervision signal, and invoke a pre-trained sentence encoder for encoding each text as $\vec{e}_{\text{s}}^{\,i} \in \mathbb{R}^{d}$. We denote the corresponding batch of semantically encoded texts as $E_{\text{s}} \in \mathbb{R}^{b\times d}$, and proceed to calculate the distance matrix $D \in \mathbb{R}^{b\times b}$ from the similarity matrix $S \in \mathbb{R}^{b\times b}$:

$$\mathcal{S} = \frac{E_{\text{s}} E_{\text{s}}^{\intercal}}{\|E_{\text{s}}\|^{2}}, \qquad \mathcal{D} = 1 - \mathcal{S}, \tag{9}$$

We rely on $\mathcal{D}$ in order to re-scale $\mathcal{V}$ by:

$$\mathcal{V}_{\mathcal{D}} = \mathcal{V} \odot \mathcal{D}, \quad \text{where} \quad \mathcal{V}_{\mathcal{D}} \in \mathbb{R}^{b\times b}, \tag{10}$$

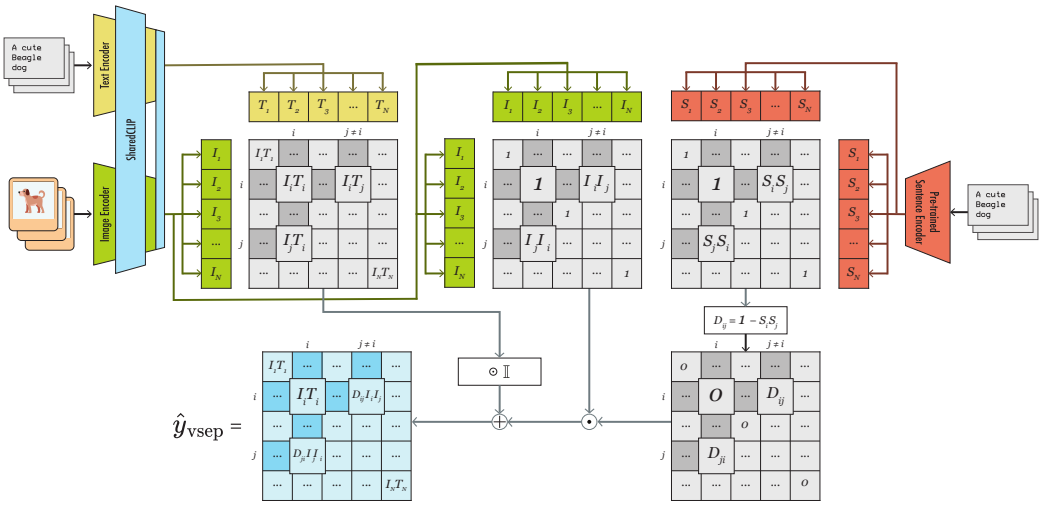

Figure 3: Schematic summary of the Intra-Modality Separation approach in AlignCLIP.

and $\odot$ denotes the element-wise product. The re-scaling mechanism encourages reducing the dot product values in $\mathcal{V}$ for semantically similar images, while increasing it for dissimilar images.

Afterwards, for calculating the logits of positive samples, we calculate $\mathcal{M} = E_{\text{v}} E_{\text{t}}^{\intercal}$ and mask the non-diagonal values by $\text{diag}(\mathcal{M}) = \mathbb{I} \odot \mathcal{M}$. We then obtain the $\hat{y}_{\text{vsep}}$ logits by:

$$\hat{y}_{\text{vsep}} = \exp(\tau) \cdot [\text{diag}(\mathcal{M}) + \mathcal{V}_{\mathcal{D}}], \quad \hat{y}_{\text{vsep}} \in \mathbb{R}^{b \times b}. \tag{11}$$

In Figure 3, our approach for obtaining IMSep is schematically summarized. Ultimately, we define the Intra-Modality Separation loss as:

$$\mathcal{L}_{\text{IMsep}} = H(\hat{y}_{\text{vsep}}, Y), \tag{12}$$

and adopt the core of the CLIP loss to represent the cross-modal separation:

$$\mathcal{L}_{\text{CRsep}} = H(\hat{y}_{\text{v}}, Y) + H(\hat{y}_{\text{t}}, Y). \tag{13}$$

The final loss function optimized in AlignCLIP is:

$$\mathcal{L} = \mathcal{L}_{\text{CRsep}} + \alpha \mathcal{L}_{\text{IMsep}} \tag{14}$$

Note that it is sufficient to define the Intra-Modality Separation function for only one of the modalities, image in our case, since the cross-modal objective defined by $\mathcal{L}_{\text{CRsep}}$ already behaves as a supervision for the other modality, text in our case, and enforces the Intra-Modality Separation in the opposite modality as well. To better support this statement, we extensively experiment on the effects of adding a similar Intra-Modality Separation on text embeddings in Section A.3 and show that it is sufficient to impose the Intra-Modality Separation on the image embeddings.

4 Experiments

4.1 Training Dataset and Setup

We used the Conceptual Caption 12M (CC12M) dataset (Changpinyo et al., 2021) for pre-training the models. In order to ensure a fair comparison of CLIP, we configured our setup for SharedCLIP and AlignCLIP to be similar to that of the original CLIP with the ViT-B-16 backend. The pre-trained semantic encoder utilized in AlignCLIP for re-scaling image–image cosine similarities is the SBERT all-mpnet-base-v2 model. For fairness in the comparisons, we trained all models from scratch using the CC12M dataset and the OpenCLIP implementation (Cherti et al., 2023; Ilharco et al., 2021). In AlignCLIP, we set $\alpha = 0.5$. Section A.2 provides more details about the training setup.

MODEL	CC3M	MSCOCO	IMAGENET-1K	CIFAR-100	CIFAR-10
CLIP	0.42	0.47	0.41	0.38	0.40
SHAREDCLIP	0.59	0.62	0.57	0.54	0.54
IMSEP	0.61	0.64	0.59	0.58	0.6
ALIGNCLIP	**0.64**	**0.67**	**0.63**	**0.62**	**0.64**

Table 1: Comparison of the alignment score.

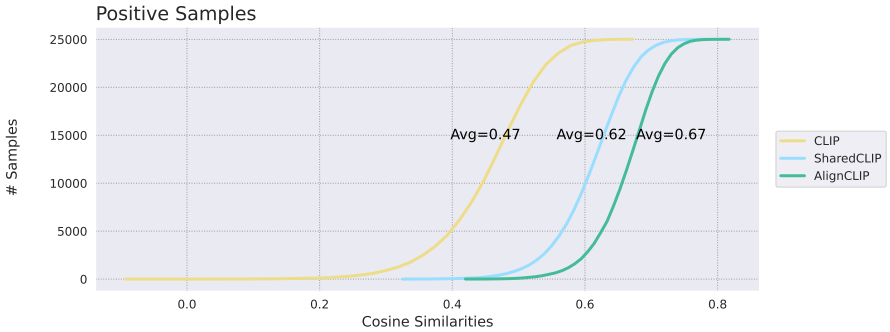

Figure 4: Cumulative distribution of pairwise cosine similarities of positive samples in MSCOCO.

4.2 CROSS-MODAL ALIGNMENT

We start by reporting and comparing the alignment scores when using CLIP, SharedCLIP, and AlignCLIP models on the validation sets from CC3M, MSCOCO as well as the ImageNet-1K, CIFAR-100, and CIFAR-10 test datasets. Table 1 summarizes the corresponding alignment scores. We observe that the original CLIP model has relatively low alignment scores, varying within $[0.38, 0.47]$, across all five datasets. In contrast, sharing the parameter space in SharedCLIP results in noticeable improvements of up to 0.17 in the alignment scores. Furthermore, using AlignCLIP yields even better alignment scores, ranging from 0.62 to 0.67. In other words, AlignCLIP reduces the average angle between the paired image–text embedding from about 70° to 47°, which can be interpreted as reducing the modality gap.

We also plot the cumulative distribution of cosine similarities of the positive samples from MSCOCO when encoded using the original CLIP, SharedCLIP, and AlignCLIP in Figure 4. We find that using SharedCLIP noticeably shifts the distribution of the cosine similarity of positive samples towards higher similarity values. A higher similarity of positive samples, i.e., image–text pairs, means achieving greater cross-modal alignment, and thus a lower modality gap. Furthermore, AlignCLIP shifts the distribution even more to the right, resulting in higher similarities of positive samples, and a better reduction of the modality gap.

For a more comprehensive comparison of the distribution of each modality and studying the modality gap, we visualize the DOSNES projection of the encoded image–texts from the MSCOCO dataset in Figure 5. As can be seen, the uni-modal embeddings of the original CLIP are densely located on opposite sides of the hypersphere. In contrast, the embeddings get spread out, hence reducing the modality gap, when using the SharedCLIP model. This observation confirms our hypothesis that sharing layers in SharedCLIP adds greater inductive bias towards a shared embedding space, in comparison to training separate transformers in CLIP, and therefore, reduces the gap. Finally, the embedding space of AlignCLIP achieves the best spread of the uni-modal embeddings and substantially decreases the gap between image and text embeddings, showing the effectiveness of pushing the image embeddings apart from each other by the IMSep loss. In summary, Table 1, Figures 4 and 5 confirm that AlignCLIP achieves an embedding space with the least sparsity, least modality gap, and the best cross-modal alignment.

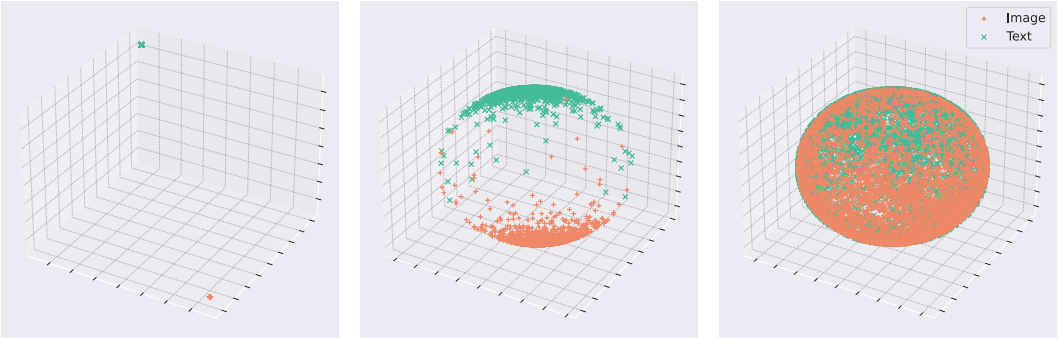

(a) Original CLIP (b) SharedCLIP (c) AlignCLIP

Figure 5: DOSNES visualization of the multi-modal embeddings using CC3M

MODEL	IMAGENET-1K		CIFAR-100		CIFAR-10		FLOWERS-102		STANFORD CARS	
	TOP1	TOP5	TOP1	TOP5	TOP1	TOP5	TOP1	TOP5	TOP1	TOP5
CLIP	31.4	58.7	28.1	55.9	61.5	95.6	18.0	39.1	11.6	36.5
SHAREDCLIP	32.1	59.7	26.4	54.7	56.9	95.2	18.2	38.9	10.7	35.4
IMSEP	32.1	58.9	31	60.1	61.6	96.2	**20.7**	**40.5**	9.3	32.7
ALIGNCLIP	**32.8**	**60.6**	**36.5**	**66.4**	**69.3**	**97.8**	18.8	40.3	**11.8**	**38.1**

Table 2: Accuracy scores for zero-shot image classification.

4.3 CLASSIFICATION

CLIP's pre-training objective resulted in outstanding image classification performance when tested in either zero-shot or linear probing settings (Radford et al., 2021). Therefore, we further assess the performance of SharedCLIP and AlignCLIP in classification tasks.

Zero-Shot Image Classification. We conduct zero-shot classification experiments on ImageNet-1K (Russakovsky et al., 2015), CIFAR-100, CIFAR-10 (Krizhevsky et al., 2009), Flowers-102 (Nilsback & Zisserman, 2008), and Stanford Cars (Krause et al., 2013), with the combination of text prompts used by CLIP (Radford et al., 2021), e.g., "a photo of the {label}". The experimental results summarized in Table 2 show that SharedCLIP improves the classification performance on the ImageNet-1K dataset and reduces the accuracy on the rest of the datasets. In contrast, AlignCLIP yields the best scores across all five datasets. It achieves 1.4% and 2% improvement of Top-1 and Top-5 accuracy, respectively, on ImageNet-1K when compared to the original CLIP. On CIFAR-10, AlignCLIP achieves up to 8% and 2% improvements in Top-1 and Top-5 accuracy scores. Similarly, using AlignCLIP for CIFAR-100 results in about 8% and 11% enhancement in Top-1 and Top-5 accuracy scores. The trend of improvement is also observed on the Flowers-102 and Stanford Cars datasets. Our experiments thus evince that via sharing parameters and the additional IMSep separation, AlignCLIP enhances the downstream zero-shot image classification task.

Linear Probing. We further test the performance of SharedCLIP and AlignCLIP when performing linear probing for image classification and report the Top-1 accuracy results in Table 3. For all datasets, we train the linear classifier layer with a batch size of 128, for 30 epochs, with AdamW optimization, and a cosine scheduler with a starting learning rate of 5×10^{-4}. Table 3 shows that SharedCLIP generally outperforms CLIP in this setting and furthermore, AlignCLIP achieves the best scores, improving the image classification task with linear probing by up to 5% in comparison to CLIP. Overall, our experiments show that AlignCLIP achieves the best classification performance in both zero-shot and linear probing settings.

4.4 ROBUSTNESS TO NATURAL DISTRIBUTION SHIFT

In the zero-shot image classification task, CLIP has additionally shown impressive robustness to natural distribution shifts and promising generalizability to out-of-distribution images. Therefore, we

MODEL	IMAGENET-1K	CIFAR-100	CIFAR-10	FLOWERS-102	STANFORD CARS
CLIP	50.0	62.6	85.0	71.5	42.2
SHAREDCLIP	51.2	63.0	85.0	74.4	40.5
IMSEP	**52.2**	65.9	86.6	**79.5**	**46.3**
ALIGNCLIP	51.5	**67.4**	**87.2**	**76.8**	**45.6**

Table 3: Accuracy scores for image classification with linear probing.

MODEL	IMAGENETV2		IMAGENET-R		IMAGENET-A		IMAGENETSKETCH	
	TOP1	TOP5	TOP1	TOP5	TOP1	TOP5	TOP1	TOP5
CLIP	27.1	53.3	39.8	65.8	6.5	25.4	19.4	41.8
SHAREDCLIP	27.5	53.5	40.2	**67.3**	6.7	25.5	20.6	**43.2**
IMSEP	27.5	53.3	40.5	**67.5**	6.7	24.5	20.2	43.1
ALIGNCLIP	**29.1**	**54.4**	**41.2**	**67.3**	**7.0**	**25.6**	**20.7**	**43.2**

Table 4: Accuracy scores for zero-shot classification and natural distribution shift.

expand our evaluations and investigate to what extent SharedCLIP and AlignCLIP are affected by natural distribution shifts. We use the ImageNetV2, ImageNet-R, ImageNet-A, and ImageNetSketch datasets for these evaluations and report the corresponding results in Table 4, in terms of Top-1 and Top-5 accuracy. It is first observed that SharedCLIP generally improves the classification accuracy in comparison to the CLIP model. Secondly, AlignCLIP achieves the best classification results across all datasets. In summary, when comparing to the CLIP model, AlignCLIP achieves about 2% improvement in Top-1 and Top-5 accuracy scores, leading to the conclusion that sharing parameters and applying IMSep in AlignCLIP improve the robustness to natural distribution shifts in comparison to the original CLIP model.

4.5 MULTI-MODAL RETRIEVAL

In addition to classification, we evaluate SharedCLIP and AlignCLIP in the applications of zero-shot and fine-tuned image-to-text and text-to-image retrieval using the MSCOCO (Lin et al., 2014) and Flickr30K (Plummer et al., 2015) datasets. In all settings, the text prompt "a photo of the {caption}" is used. When fine-tuning, the batch size was set to 128 and the AdamW optimizer with learning rate 5×10^{-6} and a weight decay of 0.2 was used.

The results of the zero-shot and fine-tuned evaluations are reported in Table 5. Our experiments show that both SharedCLIP and AlignCLIP improve the retrieval results measured by $R@\{1, 5, 10\}$ on both datasets when compared to the original CLIP model. In addition, AlignCLIP achieves the best overall results in comparison to SharedCLIP. When testing text-to-image retrieval in the zero-shot setting on the MSCOCO dataset, SharedCLIP outperforms AlignCLIP at R@10 by 1%. However, after fine-tuning, the recall difference is reduced to 0.5%. Similarly, for the image-to-text retrieval on the Flickr dataset, SharedCLIP outperforms AlignCLIP by about 1% at $R@\{1, 5\}$ and fine-tuning makes the performances marginally different.

For a more comprehensive understanding of the differences in results in the retrieval task, Figure 6A provides an example text query for which SharedCLIP achieves a higher $R@5$ image retrieval in comparison to AlignCLIP. We provide the images at rank 1-3 and observe that all models retrieve images that are semantically relevant for the query text, but might not necessarily be the ground truth. In this example, such characteristics of the dataset can particularly affect the evaluation results of AlignCLIP, due to the semantic regularization in IMSep, as it will make the semantically similar images closer to each other and can retrieve semantically close samples that are not labeled as the ground truth. We suspect that this phenomenon is more noticeable in the retrieval scenario in comparison to image classification datasets, as in the classification tasks, classes are more disjoint. In Figure 8, we further provide the ground truth texts for each image. Moreover, Figure 9 provides more of such, and Figure 10 illustrates text rankings given sample image queries.

	Model	MSCOCO						Flickr30K					
		I → T			T → I			I → T			T → I		
		R@1	R@5	R@10	R@1	R@5	R@10	R@1	R@5	R@10	R@1	R@5	R@10
ZS	CLIP	31.4	57.0	68.6	20.5	44.1	55.9	53.2	80.5	88.6	39.9	69.0	78.5
ZS	SharedCLIP	33.5	59.6	70.8	21.8	45.4	57.3	58.3	83.6	89.8	42.5	70.0	79.1
ZS	IMSep	33.7	60.8	71.4	21.5	45.2	56.8	56.8	82.3	89.2	42	69.9	79.1
ZS	AlignCLIP	35.1	60.8	71.4	21.9	45.4	56.8	57.2	82.3	89.8	42.7	70.2	79.1
FT	CLIP	39.6	67.5	78.3	26.7	53.4	65.7	64.8	87.8	93.9	47.4	75.9	84.0
FT	SharedCLIP	40.7	69.2	79.6	**27.9**	**55.0**	**66.7**	**66.5**	**89.1**	94.1	48.9	76.4	84.3
FT	IMSep	41	69.3	79.7	27.8	54.5	66.2	64.8	87.5	93.6	48.5	76.5	84.4
FT	AlignCLIP	**41.7**	**69.3**	**80.1**	**27.9**	54.8	66.2	66	**89.1**	**94.5**	**49.4**	**76.7**	**84.4**

Table 5: Zero-shot (ZS) and fine-tuned (FT) cross-modal retrieval summarized with R@{1, 5, 10}. Blue color represents the best performance in the ZS setting. Numbers in bold represent the best scores.

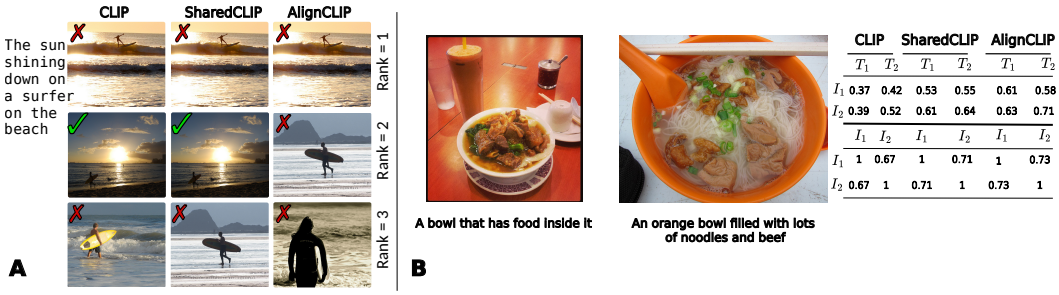

Figure 6: Qualitative analysis of the image rankings and cosine similarities on MSCOCO.

In contrary, in Figure 6B, we provide an example where AlignCLIP retrieves the most accurate caption or image. We use CLIP, SharedCLIP, and AlignCLIP to encode the images and texts, and report the cosine similarities on the right side. As can be seen, when querying the first image (on the left), the similarity of the first image and the second text (on the right) using the CLIP embeddings is higher in comparison to the ground truth caption, suggesting that the second text will, incorrectly, get selected as the predicted caption when using CLIP. This shortcoming still appears when using SharedCLIP for encoding the images and texts. However, when using AlignCLIP, the cosine similarity of the first image and the first text is higher in comparison to the second text, meaning that when querying the first image, the ground truth caption, which is semantically more correct in comparison to the second text, successfully gets selected. This suggests that the semantic regularization of the Intra-Modality Separation in AlignCLIP, which is calculated using the semantics of the text samples, potentially contributes to capturing more details in the captions, and, hence, improving the retrieval performance.

4.6 Ablation Study

This section provides an ablation study on the effectiveness of the re-scaling mechanism proposed in Eq. 10. To this end, we compare the performance of AlignCLIP with and without the re-scaling mechanism on ImageNet-1K, CIFAR-100, CIFAR-10 for zero-shot classification, ImageNetV2 for robustness to distribution shift, and the MSCOCO and Flickr30K datasets for the retrieval task. From the summarized results in Table 6, we can substantially conclude that the re-scaling mechanism is effective in controlling the separation of similar image samples in the batch, and therefore, increasing the performance of the downstream tasks.

4.7 Comparison with State-of-the-art models

Table 7 provides a comparison of SharedCLIP and AlignCLIP with the state-of-the-art CLIP-based models. One of the prominent previous studies that also reports the alignment score is the CyCLIP

MODEL	IMAGENET-1K	CIFAR-100	CIFAR-10	IMAGENETV2	MSCOCO		FLICKR	
	TOP1	TOP1	TOP1	TOP1	I → T	T → I	I → T	T → I
ALIGNCLIP-W/O RESCALING	32.8	34.7	64.2	27.9	34.0	59.7	56	42.5
ALIGNCLIP	32.8	**36.5**	**69.3**	**29.1**	**35.1**	**60.8**	**57.2**	**42.7**

Table 6: Ablation study on the re-scaling mechanism in AlignCLIP.

MODEL	IMAGENET-1K		CIFAR-100		CIFAR-10		IMAGENET-A		ALIGNMENT
	TOP1	TOP5	TOP1	TOP5	TOP1	TOP5	TOP1	TOP5	IMAGENET-1K
CLIP (RADFORD ET AL., 2021)	16.5	34.1	23.7	49.7	51.3	92.7	4	15.8	0.36
NAIVE SHIFTING (LIANG ET AL., 2022)	16.6	34.6	24.5	52.5	51.2	91.2	43.3	68.8	15.8 (WITH LAMBDA=0.5)
CYCLIP (GOEL ET AL., 2022)	15	32	21.8	48	44.7	85.4	3.3	13.6	0.32
SHAREDCLIP	17.4	**34.9**	26	52.1	57	92.9	3.7	14.5	0.45
ALIGNCLIP	17.6	**34.9**	**26.3**	**54**	**57.9**	**93.7**	**4.2**	**16.1**	**0.63**
DFSEP * (JIANG ET AL., 2023)	**20.2**	33.2	19.4	46.3	46.6	92.4	3.4	15.8	-

Table 7: Comparison with the state-of-the-art CLIP-based models. * Uses ResNet50 backend.

model (Goel et al., 2022), which is trained using the CC3M (Sharma et al., 2018) dataset. Furthermore, Jiang et al. (2023) proposes Deep Feature Separation (DFSep) objective functions that aim at improving the modality-independent information of the latent embeddings, and is also trained on CC3M. For a fair comparison with CLIP and CyCLIP, we re-train these models with the same hyperparameters as SharedCLIP and AlignCLIP. Furthermore, we train versions of SharedCLIP and AlignCLIP with the CC3M dataset and compare the resulting alignment scores as well as the downstream performance in Table 7. As for the DFSep model, we report the numbers directly from the paper Jiang et al. (2023). This model uses a ResNet50 backend for the vision encoder and the BERT model for encoding text. In contrast to the rest of the models compared in Table 7, DFSep is trained with the batch size of 128, embedding dimensionality of 1024, learning rate of 5e-4 and warmup value of 10000. Our results show a promising improvement of alignment scores while improving the downstream performance in comparison to the previous models.

5 RELATED WORK

Modifications of CLIP. Prior work has sought to improve several different aspects of CLIP, e.g., introducing a multi-positive contrastive loss in UniCLIP (Lee et al., 2022), an additional image-based contrastive loss in SLIP (Mu et al., 2022), optimizing the geometric consistency of the image and text embeddings in CyCLIP (Goel et al., 2022), proposing a non-contrastive training regimen based on image–text pairs in xCLIP (Zhou et al., 2023), employing pairwise sigmoid loss for scaling up the batch size in SigLIP (Zhai et al., 2023), and domain adaptation by refining the fine-tuning in ReCLIP (Hu et al., 2024). In contrast, AlignCLIP studies the cross-modal alignment in CLIP by investigating the effects of parameter-sharing as well as intra-modality separation.

Modality Gap in CLIP. The modality gap in CLIP was first studied by Liang et al. (2022). They showed that the modality gap is caused by a combination of the model initialization and the contrastive loss optimization. Furthermore, they attempted to study the effects of closing the gap by shifting the embeddings. In a similar study, Tyshchuk et al. (2023) measured the alignment of image and text embeddings in CLIP with a focus on isotropic properties. More recently, Schrodi et al. (2024) showed that one of the key factors contributing to both the modality gap and the bias in CLIP is the information-imbalance between the two modalities, i.e., images often have more detailed information of the scene in comparison to their corresponding text descriptions. Furthermore, Jiang et al. (2023) showed that exact modality alignment is suboptimal for downstream tasks, as the prediction error has a lower bound that is dependant on the modality information gap. As opposed to previous work, we show that naive shifting of the embeddings distorts the relative distances of the unpaired samples, and therefore, can harm the downstream performance. Furthermore, we show that under the same modality information gap, i.e., using the same training datasets, parameter sharing between the modality encoders as well as semantically-regularized separation of the uni-modal embeddings reduces the gap while improving the downstream tasks.

6 CONCLUSION

This work presents AlignCLIP, a novel framework for enhancing the cross-modal alignment in the CLIP embedding space. As opposed to previous naive gap reduction approaches that can distort the embedding structure, AlignCLIP reduces the gap by increasing the inductive bias towards shared embeddings as well semantic-regularized modifications of the latent space. We show that AlignCLIP substantially improves the cross-modal alignment and further achieves the best results for image classification, robustness to distribution shifts and improves the multi-modal retrieval performance in comparison to CLIP. Our qualitative analysis on the retrieval task demonstrates the changes of the ranking of the neighborhoods for semantically similar images.

REPRODUCIBILITY STATEMENT

We have provided the details of our training and evaluations setups in Section A.2. Clear explanations of the shortcoming of the previous naive attempts at reducing the gap has been provided in Section A.1. Furthermore, upon the acceptance of the paper, the source code for training our models and reproducing our experiments will be released.

REFERENCES

Soravit Changpinyo, Piyush Sharma, Nan Ding, and Radu Soricut. Conceptual 12m: Pushing web-scale image-text pre-training to recognize long-tail visual concepts. In *Proceedings of the IEEE/CVF Conference on Computer Vision and Pattern Recognition (CVPR)*, pp. 3558–3568, June 2021.

Mehdi Cherti, Romain Beaumont, Ross Wightman, Mitchell Wortsman, Gabriel Ilharco, Cade Gordon, Christoph Schuhmann, Ludwig Schmidt, and Jenia Jitsev. Reproducible scaling laws for contrastive language-image learning. In *Proceedings of the IEEE/CVF Conference on Computer Vision and Pattern Recognition (CVPR)*, pp. 2818–2829, June 2023.

Alexey Dosovitskiy, Lucas Beyer, Alexander Kolesnikov, Dirk Weissenborn, Xiaohua Zhai, Thomas Unterthiner, Mostafa Dehghani, Matthias Minderer, Georg Heigold, Sylvain Gelly, et al. An image is worth 16x16 words: Transformers for image recognition at scale. In *International Conference on Learning Representations*, 2020.

Shashank Goel, Hritik Bansal, Sumit Bhatia, Ryan Rossi, Vishwa Vinay, and Aditya Grover. Cyclip: Cyclic contrastive language-image pretraining. In S. Koyejo, S. Mohamed, A. Agarwal, D. Belgrave, K. Cho, and A. Oh (eds.), *Advances in Neural Information Processing Systems*, volume 35, pp. 6704–6719. Curran Associates, Inc., 2022. URL https://proceedings.neurips.cc/paper_files/paper/2022/file/2cd36d327f33d47b372d4711edd08de0-Paper-Conference.pdf.

Xuefeng Hu, Ke Zhang, Lu Xia, Albert Chen, Jiajia Luo, Yuyin Sun, Ken Wang, Nan Qiao, Xiao Zeng, Min Sun, Cheng-Hao Kuo, and Ram Nevatia. Reclip: Refine contrastive language image pre-training with source free domain adaptation. In *Proceedings of the IEEE/CVF Winter Conference on Applications of Computer Vision (WACV)*, pp. 2994–3003, January 2024.

Gabriel Ilharco, Mitchell Wortsman, Ross Wightman, Cade Gordon, Nicholas Carlini, Rohan Taori, Achal Dave, Vaishaal Shankar, Hongseok Namkoong, John Miller, Hannaneh Hajishirzi, Ali Farhadi, and Ludwig Schmidt. Openclip, July 2021. URL https://doi.org/10.5281/zenodo.5143773. If you use this software, please cite it as below.

Qian Jiang, Changyou Chen, Han Zhao, Liqun Chen, Qing Ping, Son Dinh Tran, Yi Xu, Belinda Zeng, and Trishul Chilimbi. Understanding and constructing latent modality structures in multi-modal representation learning. In *Proceedings of the IEEE/CVF Conference on Computer Vision and Pattern Recognition (CVPR)*, pp. 7661–7671, June 2023.

Jonathan Krause, Michael Stark, Jia Deng, and Li Fei-Fei. 3d object representations for fine-grained categorization. In *Proceedings of the IEEE International Conference on Computer Vision (ICCV) Workshops*, June 2013.

Alex Krizhevsky, Geoffrey Hinton, et al. Learning multiple layers of features from tiny images. 2009.

Janghyeon Lee, Jongsuk Kim, Hyounguk Shon, Bumsoo Kim, Seung Hwan Kim, Honglak Lee, and Junmo Kim. Uniclip: Unified framework for contrastive language-image pre-training. In S. Koyejo, S. Mohamed, A. Agarwal, D. Belgrave, K. Cho, and A. Oh (eds.), *Advances in Neural Information Processing Systems*, volume 35, pp. 1008–1019. Curran Associates, Inc., 2022. URL https://proceedings.neurips.cc/paper_files/paper/2022/file/072fd0525592b43da661e254bbaadc27-Paper-Conference.pdf.

Victor Weixin Liang, Yuhui Zhang, Yongchan Kwon, Serena Yeung, and James Y Zou. Mind the gap: Understanding the modality gap in multi-modal contrastive representation learning. In S. Koyejo, S. Mohamed, A. Agarwal, D. Belgrave, K. Cho, and A. Oh (eds.), *Advances in Neural Information Processing Systems*, volume 35, pp. 17612–17625. Curran Associates, Inc., 2022. URL https://proceedings.neurips.cc/paper_files/paper/2022/file/702f4db7543a7432431df588d57bc7c9-Paper-Conference.pdf.

Tsung-Yi Lin, Michael Maire, Serge Belongie, James Hays, Pietro Perona, Deva Ramanan, Piotr Dollár, and C Lawrence Zitnick. Microsoft coco: Common objects in context. In *Computer Vision–ECCV 2014: 13th European Conference, Zurich, Switzerland, September 6-12, 2014, Proceedings, Part V 13*, pp. 740–755. Springer, 2014.

Yao Lu, Jukka Corander, and Zhirong Yang. Doubly stochastic neighbor embedding on spheres. *Pattern Recognition Letters*, 128:100–106, 2019. ISSN 0167-8655. doi: https://doi.org/10.1016/j.patrec.2019.08.026. URL https://www.sciencedirect.com/science/article/pii/S0167865518305099.

Norman Mu, Alexander Kirillov, David Wagner, and Saining Xie. Slip: Self-supervision meets language-image pre-training. In *European conference on computer vision*, pp. 529–544. Springer, 2022.

Maria-Elena Nilsback and Andrew Zisserman. Automated flower classification over a large number of classes. In *2008 Sixth Indian Conference on Computer Vision, Graphics & Image Processing*, pp. 722–729, 2008. doi: 10.1109/ICVGIP.2008.47.

Bryan A. Plummer, Liwei Wang, Chris M. Cervantes, Juan C. Caicedo, Julia Hockenmaier, and Svetlana Lazebnik. Flickr30k entities: Collecting region-to-phrase correspondences for richer image-to-sentence models. In *Proceedings of the IEEE International Conference on Computer Vision (ICCV)*, December 2015.

Alec Radford, Jong Wook Kim, Chris Hallacy, Aditya Ramesh, Gabriel Goh, Sandhini Agarwal, Girish Sastry, Amanda Askell, Pamela Mishkin, Jack Clark, Gretchen Krueger, and Ilya Sutskever. Learning transferable visual models from natural language supervision. In Marina Meila and Tong Zhang (eds.), *Proceedings of the 38th International Conference on Machine Learning*, volume 139 of *Proceedings of Machine Learning Research*, pp. 8748–8763. PMLR, 18–24 Jul 2021. URL https://proceedings.mlr.press/v139/radford21a.html.

Olga Russakovsky, Jia Deng, Hao Su, Jonathan Krause, Sanjeev Satheesh, Sean Ma, Zhiheng Huang, Andrej Karpathy, Aditya Khosla, Michael Bernstein, Alexander C. Berg, and Li Fei-Fei. ImageNet Large Scale Visual Recognition Challenge. *International Journal of Computer Vision (IJCV)*, 115 (3):211–252, 2015. doi: 10.1007/s11263-015-0816-y.

Simon Schrodi, David T Hoffmann, Max Argus, Volker Fischer, and Thomas Brox. Two effects, one trigger: On the modality gap, object bias, and information imbalance in contrastive vision-language representation learning. In *ICLR 2024 Workshop on Mathematical and Empirical Understanding of Foundation Models*, 2024. URL https://openreview.net/forum?id=7QwFMLzQHH.

Piyush Sharma, Nan Ding, Sebastian Goodman, and Radu Soricut. Conceptual captions: A cleaned, hypernymed, image alt-text dataset for automatic image captioning. In Iryna Gurevych and Yusuke Miyao (eds.), *Proceedings of the 56th Annual Meeting of the Association for Computational Linguistics (Volume 1: Long Papers)*, pp. 2556–2565, Melbourne, Australia, July 2018. Association for Computational Linguistics. doi: 10.18653/v1/P18-1238. URL https://aclanthology.org/P18-1238.

Kirill Tyshchuk, Polina Karpikova, Andrew Spiridonov, Anastasiia Prutianova, Anton Razzhigaev, and Alexander Panchenko. On isotropy of multimodal embeddings. *Information*, 14(7), 2023. ISSN 2078-2489. doi: 10.3390/info14070392. URL https://www.mdpi.com/2078-2489/14/7/392.

Ashish Vaswani, Noam Shazeer, Niki Parmar, Jakob Uszkoreit, Llion Jones, Aidan N Gomez, Ł ukasz Kaiser, and Illia Polosukhin. Attention is all you need. In I. Guyon, U. Von Luxburg, S. Bengio, H. Wallach, R. Fergus, S. Vishwanathan, and R. Garnett (eds.), *Advances in Neural Information Processing Systems*, volume 30. Curran Associates, Inc., 2017. URL https://proceedings.neurips.cc/paper_files/paper/2017/file/3f5ee243547dee91fbd053c1c4a845aa-Paper.pdf.

Tongzhou Wang and Phillip Isola. Understanding contrastive representation learning through alignment and uniformity on the hypersphere. In Hal Daumé III and Aarti Singh (eds.), *Proceedings of the 37th International Conference on Machine Learning*, volume 119 of *Proceedings of Machine Learning Research*, pp. 9929–9939. PMLR, 13–18 Jul 2020. URL https://proceedings.mlr.press/v119/wang20k.html.

Haoxuan You, Luowei Zhou, Bin Xiao, Noel Codella, Yu Cheng, Ruochen Xu, Shih-Fu Chang, and Lu Yuan. Learning visual representation from modality-shared contrastive language-image pre-training. In *European Conference on Computer Vision*, pp. 69–87, 2022.

Xiaohua Zhai, Basil Mustafa, Alexander Kolesnikov, and Lucas Beyer. Sigmoid loss for language image pre-training. In *Proceedings of the IEEE/CVF International Conference on Computer Vision (ICCV)*, pp. 11975–11986, October 2023.

Jinghao Zhou, Li Dong, Zhe Gan, Lijuan Wang, and Furu Wei. Non-contrastive learning meets language-image pre-training. In *Proceedings of the IEEE/CVF Conference on Computer Vision and Pattern Recognition (CVPR)*, pp. 11028–11038, June 2023.

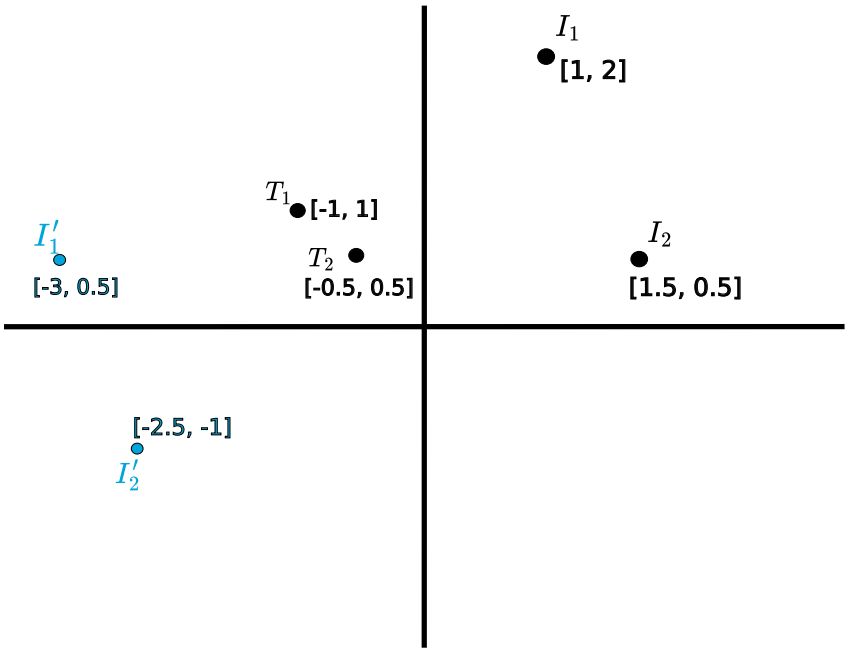

Figure 7: A 2D example illustrating that naive embedding shifts can distort the relative distance of the unpaired images and texts.

A Appendix / Supplemental Material

A.1 Destructive effects of naive embeddings translation for closing the gap

In this section, we provide a 2D example for showing how the translation proposed in Liang et al. (2022) (and later adopted in Schrodi et al. (2024)) is not guaranteed to maintain the relative distances of the *unpaired* image–text samples, and therefore, can distort the meaningful structure of the embedding space. Figure 7 provides 2 image–text pairs, i.e., (T_1, I_1) and (T_2, I_2). As derived in Eq. 15, the distance of the first image is closest to the first text, and the distance of the second image is closest to the second text. However, in Eq. 16, after shifting by Δ, as proposed by Liang et al. (2022), the distances of the second text to either of the images become equal and fail to maintain the relative distances after the shift. As a result, in downstream tasks, e.g., image retrieval given T_2, both I_1 and I_2 will be retrieved, which is incorrect.

$$\begin{aligned}
d_{1,1} &= \|T_1 - I_1\| = \|[-2,-1]\| = \sqrt{4+1} = \sqrt{5} \\
d_{1,2} &= \|T_1 - I_2\| = \|[-2.5,0.5]\| = \sqrt{6.25+0.25} = \sqrt{6.5} \\
d_{2,1} &= \|T_2 - I_1\| = \|[-1.5,-1.5]\| = \sqrt{2.25+2.25} = \sqrt{4.5} \\
d_{2,2} &= \|T_2 - I_2\| = \|[-2,0]\| = \sqrt{4+0} = \sqrt{4} \\
& d_{1,1} < d_{1,2}, \quad d_{2,2} < d_{2,1}
\end{aligned} \tag{15}$$

$$\begin{aligned}
\Delta = (T_1 + T_2) - (I_1 + I_2) &= [-1.5, 1.5] - [2.5, 2.5] = [-4, -1.5] \\
I'_1 = I_1 + \Delta = [-3, 0.5] \quad & I'_2 = I_2 + \Delta = [-2.5, -1] \\
d'_{1,1} &= \|T_1 - I'_1\| = \|[2,0.5]\| = \sqrt{4+0.25} = \sqrt{4.25} \\
d'_{1,2} &= \|T_1 - I'_2\| = \|[1.5,2]\| = \sqrt{2.25+4} = \sqrt{6.25} \\
d'_{2,1} &= \|T_2 - I'_1\| = \|[2.5,0]\| = \sqrt{6.25} \\
d'_{2,2} &= \|T_2 - I'_2\| = \|[2,1.5]\| = \sqrt{4+2.25} = \sqrt{6.25} \\
& d'_{1,1} < d'_{1,2}, \quad d'_{2,1} = d'_{2,2}
\end{aligned} \tag{16}$$

A.2 Training Dataset and Setup

For pre-training, we used the CC12M dataset (Changpinyo et al., 2021). We adopted a transformer encoder consisting of 12 layers and 12 heads in CLIP, SharedCLIP, and AlignCLIP. The same input pre-processing and augmentations employed in CLIP have been used for SharedCLIP as well as AlignCLIP, including random cropping of images to the size 224×224. The image patch size for encoding visual data is set to 16×16. When encoding texts, the maximum sequence length is set to 77 tokens and the vocabulary size for the embedding layer is set to 49,408. The output embedding dimensionality for both the vision and language modalities is set to 768. We chose our setup to be quite similar to that of the original CLIP with the ViT-B-16 backend, in order to ensure a fair comparison of CLIP and our proposed model. The SBERT all-mpnet-base-v2 model has been utilized in AlignCLIP for re-scaling image–image cosine similarities in Eq. 10.

In order to fairly compare the effectiveness of each model, we trained all of the models from scratch using the CC12M dataset and the OpenCLIP implementation (Cherti et al., 2023; Ilharco et al., 2021). For all models, we used AdamW optimization with a starting learning rate of 1×10^{-3}, cosine scheduler, 10,000 warmup steps, and a weight decay of 0.1. The initial temperature value for all models were set to 0.07. Each model was trained using an NVIDIA H100 GPU with batch size 512 for 30 epochs. We used the checkpoint from the last epoch in our evaluations of downstream experiments. In AlignCLIP, we set $\alpha = 0.5$.

A.3 Effects of text embedding separation

In Section 3.2, we proposed IMSep to enforce Intra-Modality Separation among the image embeddings. An alternative scenario could be to enforce the separation amongst the text embeddings, or even, to enforce the separation inside the image embeddings as well as the text embeddings. To examine these alternatives, we trained versions of AlignCLIP without image–image separation, instead introducing a text–text separation, which we refer to as AlignCLIP-TT. We also used the re-scaling mechanism described in Eq. 10. Furthermore, we trained a version including both image-image embeddings separation and text-text embeddings separation, i.e., AlignCLIP-II-TT. We followed the same experimental setup as described in Section A.2 and compare the results for zero-shot image classification as well as linear probing in Tables 8 and 9, respectively. As can be seen, imposing the Intra-Modality Separation merely on the image embeddings yields the best results.

Model	ImageNet-1K		CIFAR-100		CIFAR-10		Flowers-102		Stanford Cars	
	Top1	Top5	Top1	Top5	Top1	Top5	Top1	Top5	Top1	Top5
AlignCLIP (TT)	31.1	58.6	31.5	60.9	64.8	95.5	18.7	39.5	10.0	36.4
AlignCLIP (II)	**32.8**	**60.6**	**36.5**	**66.4**	**69.3**	**97.8**	**18.8**	**40.3**	**11.8**	**38.1**
AlignCLIP (II-TT)	32.4	60.0	31.2	61.8	66.4	96.9	18.7	39.9	11.8	37.1

Table 8: Accuracy scores for zero-shot image classification.

Model	ImageNet-1K	CIFAR-100	CIFAR-10	Flowers-102	Stanford Cars
AlignCLIP (TT)	51.2	64.5	86.3	74.3	41.6
AlignCLIP (II)	**51.5**	**67.4**	**87.2**	**76.8**	**45.6**
AlignCLIP (II-TT)	50.3	63.4	85.8	72.2	42.2

Table 9: Accuracy scores for image classification with linear probing.

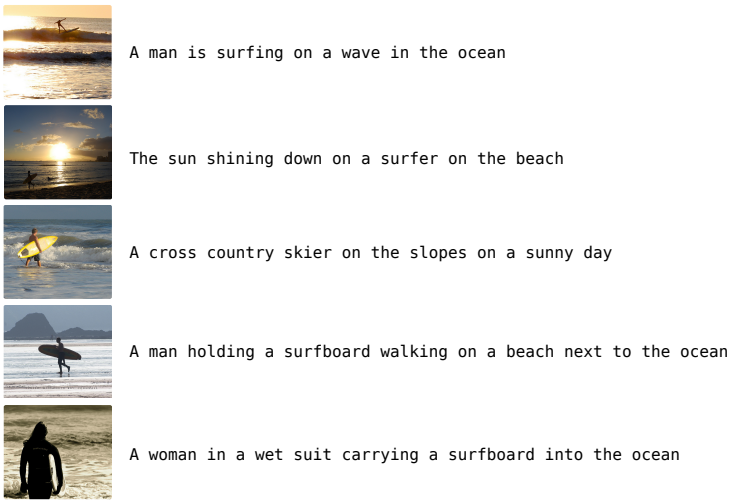

Figure 8: Ground truth texts for the Top-3 retrieved images in Figure 6.

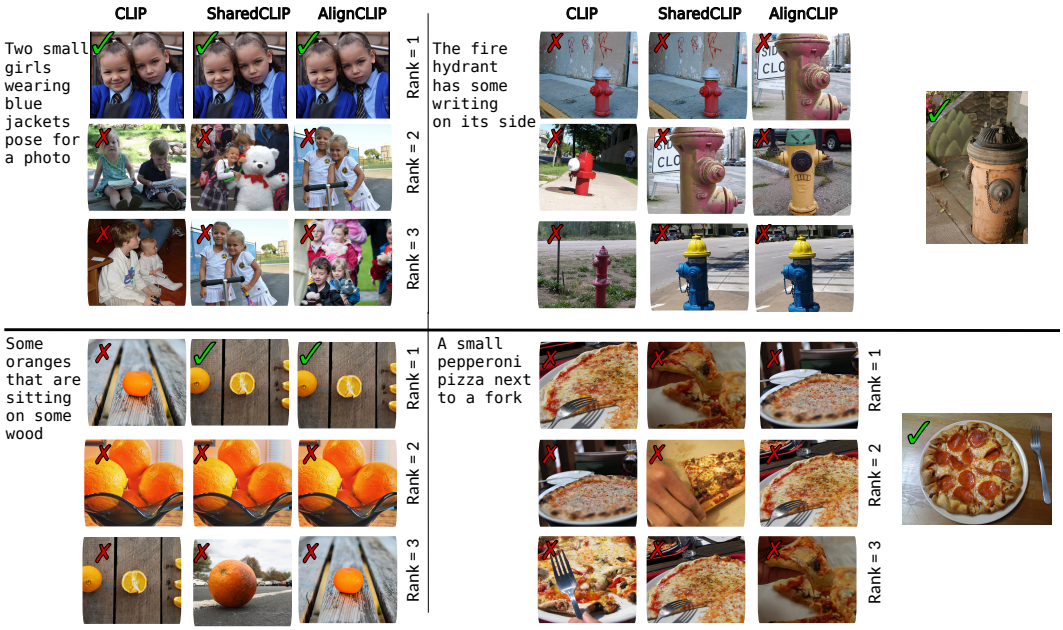

Figure 9: Qualitative analysis of the image rankings.

A.4 Qualitative Examples

In this section, further qualitative examples are provided. Figure 8 provides the ground truth text for the Top-3 images retrieved in Figure 6. Figure 9 provides further examples of the rankings when querying texts. Moreover, Figure 10 illustrates the text rankings when an image is queried.

A.5 Trend of the Temperature Value

In this section, we provide the analysis of the learned temperature value in each of the CLIP, SharedCLIP and AlignCLIP models. We have traced the value of $\frac{1}{\tau}$ and proved the plots in Figure 11.

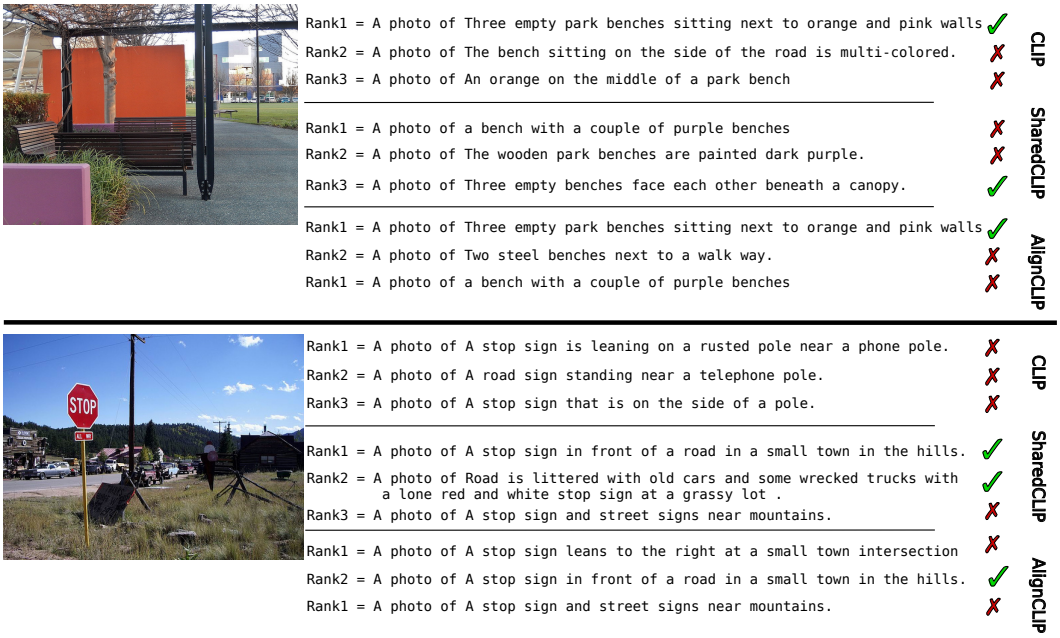

Figure 10: Qualitative analysis of the text rankings given image queries.

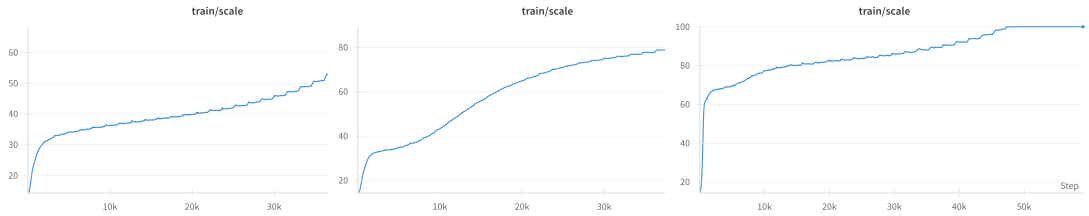

(a) Original CLIP (b) SharedCLIP (c) AlignCLIP

Figure 11: Trend of learnable the temperature value: Y-Axis shows the value of $\frac{1}{\tau}$ and X-Axis shows the step number.

A.6 Experimental results using the ViT-S-16 Transformer

In this section, we provide the results of using AlignCLIP with the ViT-S-16 backend in Tables 10-13.

MODEL	CC3M	MSCOCO	IMAGENET-1K	CIFAR-100	CIFAR-10
CLIP	0.4	0.44	0.38	0.58	0.36
SHAREDCLIP	0.58	0.61	0.57	0.56	0.57
ALIGNCLIP	**0.67**	**0.69**	**0.66**	**0.64**	**0.65**

Table 10: Comparison of the alignment score with ViT-S-16.

MODEL	IMAGENET-1K		CIFAR-100		CIFAR-10		FLOWERS-102		STANFORD CARS	
	TOP1	TOP5	TOP1	TOP5	TOP1	TOP5	TOP1	TOP5	TOP1	TOP5
CLIP	30.5	57.7	25.3	551.	57.5	94.9	16.8	37.6	9.2	32
SHAREDCLIP	29.8	56.5	27.6	56.7	61.3	95.8	17.7	37	8.8	30.9
ALIGNCLIP	**30.8**	**57.8**	**27.8**	**57.5**	**63.2**	**95.9**	**20.6**	**38.8**	**9.5**	**32.9**

Table 11: Accuracy scores for zero-shot image classification with ViT-S-16.

MODEL	IMAGENETV2		IMAGENET-R		IMAGENET-A		IMAGENETSKETCH	
	TOP1	TOP5	TOP1	TOP5	TOP1	TOP5	TOP1	TOP5
CLIP	26.1	52	36.3	63	5.7	22.4	18	**39.6**
SHAREDCLIP	25.1	50.3	36.5	62.8	5.4	22.2	18	**39.6**
ALIGNCLIP	**26.4**	**52.4**	**38.1**	**64.5**	**6.3**	**23.4**	**18.6**	**39.6**

Table 12: Accuracy scores for zero-shot classification and natural distribution shift with ViT-S-16.

	MODEL	MSCOCO						FLICKR30K					
		I → T			T → I			I → T			T → I		
		R@1	R@5	R@10	R@1	R@5	R@10	R@1	R@5	R@10	R@1	R@5	R@10
ZS	CLIP	30.4	56.9	67.4	19.9	42	53.7	52.1	77.9	85.8	38.2	66	76.1
	SHAREDCLIP	31.3	57	68.1	20.3	42.2	54.1	52.1	80.9	87.4	38.6	66.4	76.1
	ALIGNCLIP	31.8	57.1	68.1	19.9	42.2	53.9	52.7	80.6	87.2	38.7	66.6	76.4
FT	CLIP	38.2	66	76.3	25	50.5	62.8	61	84.8	91.1	45.2	72.1	82
	SHAREDCLIP	38.5	66	**76.8**	25.2	**51.1**	**63.4**	**61.1**	85.1	**91.7**	45.4	**73.4**	**82.2**
	ALIGNCLIP	**39**	**66.8**	76.4	**25.4**	50.8	63	**61.1**	**85.4**	91.6	**45.5**	72.8	82

Table 13: Zero-shot (ZS) and fine-tuned (FT) cross-modal retrieval summarized with R@{1, 5, 10}. Blue color represents the best performance in the ZS setting. Numbers in bold represent the best scores with ViT-S-16.

B LIMITATIONS

For the zero-shot classification experiments, we have tested the models using the ImageNet-1k, CIFAR-10, CIFAR-100, Stanford Cars, and Flower-102 datasets. Further classification analysis using benchmark datasets such as Hateful Memes has thus far not been conducted in this work. Moreover, this study is limited to the English language and should be followed up by further analyses on multilingual and cross-lingual representation learning. Additionally, the re-scaling mechanism in the intra-modality separation loss is dependant on the choice of pre-trained sentence encoder and has not been extensively benchmarked in this work. Pre-trained image encoders could as well be explored for providing the semantic supervision for the re-scaling mechanism.

C IMPACT STATEMENT

This paper presents research seeking to advance the field of machine learning at a fundamental level with regard to cross-modal representation learning. We acknowledge that this line of work has a broad range of potential societal implications. For instance, vision–language models may exhibit harmful biases and stereotypes, particularly when trained on data crawled from the Web. Due to their incorporation in prominent generative AI models, vision–language models may also contribute toward the model's ability to produce images portraying trademarked characters or notable figures. These sorts of concerns need to be carefully considered before incorporating such models into real-world applications.